6a
12R

CORRELATION OF PRESSURE LOSSES IN SMALL BORE TUBING FOR REYNOLDS NUMBERS BETWEEN 400 AND 50,000

A THESIS

Presented to

the Faculty of the Graduate Division

by

Gerald L. Lattal

In Partial Fulfillment

of the Requirements for the Degree

Master of Science in Aeronautical Engineering

Georgia Institute of Technology

June, 1960

"In presenting the dissertation as a partial fulfillment of the requirements for an advanced degree from the Georgia Institute of Technology, I agree that the Library of the Institution shall make it available for inspection and circulation in accordance with its regulations governing materials of this type. I agree that permission to copy from, or to publish from, this dissertation may be granted by the professor under whose direction it was written, or, in his absence, by the dean of the Graduate Division when such copying or publication is solely for scholarly purposes and does not involve potential financial gain. It is understood that any copying from, or publication of, this dissertation which involves potential financial gain will not be allowed without written permission.

_____

_____

CORRELATION OF PRESSURE LOSSES

IN SMALL BORE TUBING FOR REYNOLDS NUMBERS

BETWEEN 400 AND 50,000

Approved:

Date Approved by Chairman: June 1, 1960

ACKNOWLEDGMENTS

The author is deeply indebted to Doctor Arnold L. Ducoffe for his suggestion of the topic, and for his invaluable assistance rendered during the experimentation. Gratitude is also extended to Doctor Frank M. White for his assistance in correlating the data, and to Doctor Charles W. Gorton for his critical review of the topic. The work of Mr. George Cook in fabricating the equipment, and the assistance of Messrs. George Stone, David Pirie, and George Brown during the experimentation and in the reduction and presentation of the data, are also appreciated.

Sincere appreciation is extended to the Sandia Corporation, whose financial and material aid made this work possible.

TABLE OF CONTENTS

LIST OF TABLES

LIST OF FIGURES

LIST OF SYMBOLS

English

A	Cross-sectional area of test tubing
A_1	Area of pipe containing the orifice plate
A_2	Orifice area
al	Alcohol
B	Ratio of orifice diameter to pipe inside diameter, $\frac{D_2}{D_1}$
C	Constant
D	Test tubing diameter
D_1	Entrance pipe diameter
D_2	Orifice diameter
E	Thermal expansion coefficient
F	Correlation friction factor
f	Local friction factor
$\bar{f}$	Mean or average friction factor
f*	Pseudo friction factor
G	Mass flow per unit area
g	Gravitational constant
Hg	Mercury
K	Discharge coefficient
L	Tubing length
mm	Pressure in millimeters
n	Constant
P_1	Static pressure upstream of orifice plate

P_2	Static pressure downstream of orifice plate
p_1	Static pressure in entrance pipe upstream of test tube
p_2	Static pressure in exit pipe downstream of test tube
p_I	Static pressure at x_I
p_{II}	Static pressure at x_{II}
p_i	Transient input pressure
p_r	Transient response pressure
psig	Gauge pressure in pounds per square inch
R	Gas constant for air
Rey	Reynolds number, $Rey = wD/\mu A$
T	Static temperature
t	Time
V	Sensing volume
v	Velocity
v_1	Velocity upstream at orifice plate
v_2	Velocity downstream at orifice plate
w	Mass flow
x_I	Longitudinal position near upstream end of test tube
x_{II}	Longitudinal position near downstream end of test tube
Y	Compressibility factor

Greek

ΔP	Pressure difference across the orifice plate
Δp	Pressure difference across the test tube
μ	Coefficient of viscosity
Ω	Flow factor, $(\sqrt{^\circ R}/\text{sec.})$

ρ	Density
τ_w	Wall shearing stress

SUMMARY

The purpose of this investigation was to determine steady state friction factors in small bore tubing for Reynolds numbers between 400 and 50,000. The friction factors obtained (which were called pseudo friction factors), not only incorporated the wall friction, but also development losses, inlet and exit losses, and compressibility effects.

The experiments were run at room temperature for various system geometries using tube length and tube diameter as variables. Three tubing lengths, 60, 120, and 180 inches with five inside diameters, 0.122, 0.178, 0.259, 0.290, and 0.384 inches were investigated. Each configuration was also tested with 90, 80, and 70 per cent reduction fittings inserted at the tubing extremities.

The pseudo friction factors were computed using a theory based on the assumptions of one-dimensional, steady, continuum flow through constant area tubing, with isothermal changes of state. The equations were developed by integrating the momentum equation over a small control volume.

The results of the experiment were correlated to the Hagen-Poiseuille curve for laminar flow for straight tubes with and without reduction fittings, and to the Karman-Nikuradse curve for straight tubes without reduction fittings in turbulent flow. A method for correlating the reduction fitting data in turbulent flow was not developed in this study.

CHAPTER I

INTRODUCTION

The measurement of friction factors in small bore tubes has been the subject of experimentation for many years. The theoretical work of Karman (1) and the experiments of Nikuradse (2) have produced friction factor data in the turbulent flow regimes. Schlicting (3) has compiled data for friction factors in the laminar flow regimes. The friction factors thus far obtained were based on fully developed flow within the tube.

These friction factors, for fully developed flow, are approximated by the relation:

$$4f = C(Rey)^{-n} \qquad (I\text{-}1)$$

where f is the local value of the wall friction within the tube. This relation has the well-known form,

$$4f = 64/Rey \qquad (I\text{-}2)$$

for laminar flow from the solution of the Hagen-Poiseuille equation (4). There are many forms of the friction factor relationship for turbulent flow in smooth tubes. Blasius (5) suggested

$$4f = 0.3164(Rey)^{-1/4} \qquad (I\text{-}3)$$

which may be used to predict friction factors with reasonable accuracy for Reynolds numbers from 3,000 to 100,000. Another relation to be used

in the range of Reynolds numbers from 3,000 to 3,000,000 was presented by Drew (6) and is given by

$$4f = 0.0056 + 0.500(Rey)^{-0.32} \qquad (I\text{-}4)$$

The most accurate of these relations is the well-known semi-empirical equation, valid for all Reynolds numbers above 3,000, obtained by Karman and improved by Nikuradse which is

$$1/\sqrt{4f} = 2.0 \log_{10}(Rey\sqrt{4f}) - 0.8 \qquad (I\text{-}5)$$

Recently, a theory (7) assuming a quasi-steady, fully-developed, compressible, isothermal tube flow for predicting pneumatic pressure lag in simple series systems has been developed. The simple series system (Fig. 1) consists of constant area tubing attached to a sensing volume.

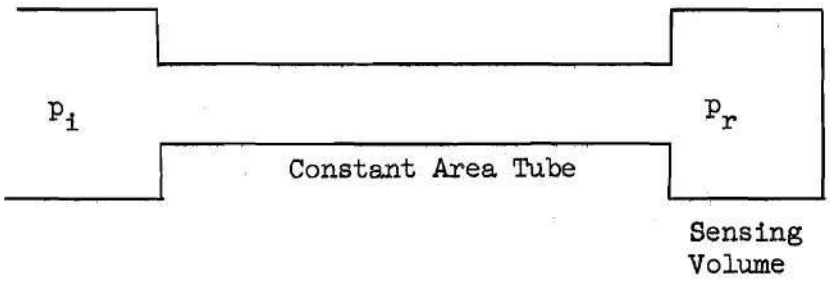

Fig. 1 Equivalent Transient System

The governing differential equation is:

$$\frac{dp_r}{dt} = \frac{\pi}{4} \frac{(RT)^{\frac{(1-n)}{(2-n)}}}{(C\mu^n)^{\frac{1}{2-n}}} \frac{D^{\frac{(5-n)}{(2-n)}}}{L^{\frac{1}{(2-n)}} V} (p_i^2 - p_r^2)^{\frac{1}{2-n}} \qquad (I\text{-}6)$$

where p_r is the response pressure in the sensing volume, R is the gas constant, T is the temperature of the air in the system, L is the tube length, D is the tube diameter, μ is the viscosity coefficient, V the sensing volume, and p_i is the input pressure. The constants C and n are determined from a friction factor relationship. It is seen from Figure 1 that the friction factors obtained previously are inadequate since the pressure taps are not located in the constant area tube in the fully developed flow regime. Therefore, a new friction factor called a pseudo friction factor (f*) will be determined, which will be approximated by a relation such as Equation (I-1) where a new C and n will be used. This pseudo friction factor will not only incorporate the wall friction within the tube, but also compressibility effects, inlet and exit losses, and development losses. Since the transient theory assumed quasi-steady flow, it is supposed that friction factors based on steady flow experiments can be used.

The data of Bradley (8) and Laster (9) have been used in this study to obtain pseudo friction factors in the Reynolds number range between 10,000 and 100,000 (purely turbulent flow). The geometries investigated by Bradley and Laster were tube lengths of 10, 15, and 19.5 feet with inside diameters of 0.180, 0.308, 0.402, and 0.524 inches.

The purpose of this investigation will be to extend the work of Bradley and Laster by considering additional tube lengths and diameters in the Reynolds number range between 400 and 50,000. In addition, the effect of reduction fittings (having diameters of 90, 80, and 70 per cent of the tube diameter) inserted at the extremities of the tubes will be determined.

The experimental data will be correlated by removing the losses added into the pseudo friction factor and comparing the results with the classical curves of Hagen-Poiseuille and Karman-Nikuradse. The final result will be a procedure for determining C and n in the relation

$$4f^* = C(Rey)^{-n} \qquad (I\text{-}7)$$

for both laminar and turbulent flow.

CHAPTER II

APPARATUS

A schematic sketch of the complete apparatus and its components is shown in Figure 2. The pressure source is connected to the system by means of 3/4-inch copper tubing with metering valves inserted between the pressure source and the test system. Flanged two inch steel pipe connected the main components of the system. The pressure taps were placed as shown in Figure 2, and were connected to the pressure measuring devices by means of 1/4-inch copper tubing. The following is a detailed description of the system components.

Pressure Source.--Two 1,000 cubic feet tanks (not shown in Figure 2), connected in series, and pressurized to a maximum of 125 psig by means of a 75 horsepower single-cycle compressor were used as the pressure source. A surge tank, held at a constant pressure of 15 psig by means of a pressure regulator, was placed between the system and the two pressure tanks.

Metering Orifices.--Flow rates were determined (see Appendix) using ASME (10) standard, sharp-edged, metering orifices having B ratios of 0.1 and 0.05, where B is the ratio of the metering orifice diameter to the pipe inside diameter (D_2/D_1). Flange taps were employed to determine the pressure drop across the orifice plate which was constructed from stainless steel. The orifice plate with $B = 0.1$ was used in conjunction with test tubing having diameters of 0.384 inches and 0.290 inches; whereas, the orifice plate with $B = 0.05$ was used with the tubing dia-

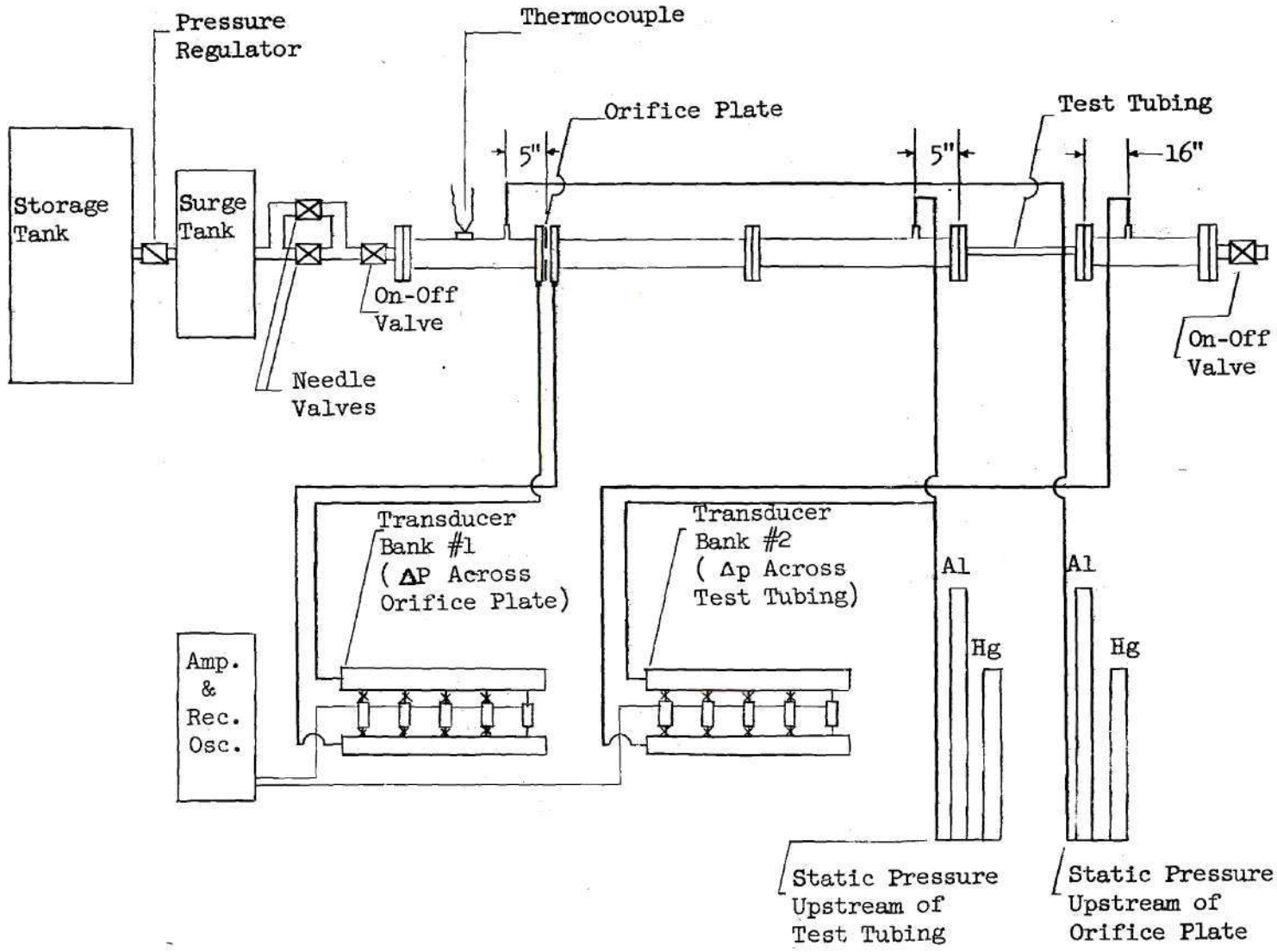

Fig. 2 Schematic of Test Apparatus

meters of 0.259 inches, 0.178 inches and 0.122 inches.

Pressure Measurements.--An alcohol manometer (0-1100 mm al range) and a mercury manometer (0-1500 mm Hg range) were used to measure static pressures upstream of the orifice plate. The alcohol manometer was clamped off when its maximum pressure was reached. A similar arrangement was used to obtain static pressures upstream of the test tube.

The difference in pressure across the orifice plate was measured by a bank of five differential transducers. For simplicity they will be called A_1, B_1, C_1, D_1, and E_1. Their respective ranges are shown in Table 1. At the start of each run (low mass flow) only transducer A_1 appeared on the record trace. As A_1 approached its maximum pressure, B_1 would appear on the record trace. As A_1 reached its maximum allowable pressure it was isolated from the system by means of shut-off valves and B_1 commenced to record pressures by itself. Thus, an overlap between transducers was provided, and gave added sensitivity and reasonable accuracy. An identical procedure was performed between B_1 and C_1 and so forth. A similar bank of differential transducers (denoted by A_2, B_2, C_2, D_2, and E_2) was used to measure pressure differences across the test tube.

All transducers were calibrated with micro-manometers. For the most sensitive transducers (A, B, and C), the micro-manometers were filled with a low viscosity oil (specific gravity = 0.827), while mercury was used for transducers D and E.

Power Supplies and Recording Equipment.--The electronic recording equipment consisted of two oscillator-power supply combinations, ten separate amplifiers, and a recording oscillograph.

Table 1. Transducer Pressure Ranges

Differential Transducer	Pressure Range mm oil*	mm Hg
A_1	0 - 125	0 - 7.6
B_1	100 - 425	6.1 - 25.8
C_1	360 - 710	21.9 - 43.2
D_1		39 - 103
E_1		90 - 510
A_2	0 - 125	0 - 7.6
B_2	100 - 425	6.1 - 25.8
C_2	360 - 710	21.9 - 43.2
D_2		39 - 103
E_2		90 - 510

*Note: Specific gravity of oil = 0.827

The oscillator-power supply provided the filament current, the regulated plate voltage, and a three kilocycle carrier frequency for the amplifiers. The power supply also supplied the exciting voltage for the differential pressure transducers.

The output signals from the ten pressure transducers were fed into separate amplifiers. The basic components of each amplifier were the balancing portion of the transducer bridge network, an attenuator, a three kilocycle carrier amplifier, and a demodulator.

The output signals from the ten amplifiers were impressed on separate galvanometers in the recording oscillograph. The optical distance from the galvanometers to the recording film was 11.5 inches. The recording film was stored in spool-type magazines and was run at an approximate speed of 1.8 inches per second.

Temperature Records.--A thermocouple (placed as shown in Figure 2) and potentiometer system was used to measure the static temperature of the air in the system. The temperatures were read (within one degree) directly from a needle gauge on the potentiometer.

Test Tubing and Fittings.--The test tubes used were commercially bought seamless steel tubes. Three lengths of tubing, 60, 120, and 180 inches, each with five inside diameters, 0.122 inches, 0.178 inches, 0.259 inches, 0.290 inches and 0.384 inches, were tested (tabulated in Table 2). The fittings used were turned from aluminum and steel tubes, and bored so that their inside diameters were 90, 80, and 70 per cent of each respective test tube diameter. The test tubes were integrated into the system with 37 degree flare fittings.

Valves.--The flow rates were controlled by two valves, (one a sensitive

Table 2. Test Tubes Investigated*

Length (inches)	Inside Diameter (inches)	L/D Ratio
60	0.178	334
60	0.259	234
60	0.290	210
60	0.384	159
120	0.122	984
120	0.178	674
120	0.259	465
120	0.290	416
120	0.384	315
180	0.122	1475
180	0.178	1011
180	0.259	697
180	0.290	624
180	0.384	472

*Note: All tubes investigated were tested with 100, 90, 80, and 70 per cent reduction fittings.

micrometer needle valve for low flow rates, and the other a coarse needle valve for higher rates), arranged in parallel.

Rubber diaphragm shut-off valves were placed at the entrance and exit of the system to facilitate checking for leaks.

CHAPTER III

PROCEDURE

The main steps of the daily test procedure began with the calibration of the differential transducers. Following the calibrations, the two 1,000 cubic foot tanks were pumped to a pressure of approximately 125 psig and the surge tank pressure regulated to 15 psig. Prior to each test run, the system was checked for leaks by pressurizing it to 15 psig and closing the valves at the entrance and exit.

The details of the main steps are included in the following description of the test procedure.

Calibration of Differential Transducers.--Transducers A, B, and C were calibrated using the oil micro-manometer, sensitive to approximately $\pm$ 0.1 mm oil ($\pm$ 0.006 mm Hg). Transducers D and E were calibrated with the mercury micro-manometer which is sensitive to approximately $\pm$ 0.05 mm Hg. The pressure ranges covered by the transducers are shown in Table 1.

Test Run.--A test run was performed by opening the micrometer needle valve slowly to allow air to flow through the system. At appropriate mass flow intervals, with steady flow established, records were taken. As each oscillograph trace was recorded, the static pressures upstream of the orifice plate and test tube were read from the alcohol or mercury manometers and recorded. For large flow rates the less sensitive needle valve was used as a flow regulator. Also, as the differential pressure range of each transducer was exceeded, it was isolated from the system

and the subsequent transducer allowed to record as described previously. The temperature of the air in the system was recorded at various times during the test run. This procedure was continued until the flow rate was such as to choke the flow of air through the test tube. The downstream exit pressure was constant at atmospheric pressure.

Accuracy.--The error in the experimental data is essentially that of the accuracy of the calibrations, plus the human error in reading the oscillograph records. The calibration curves taken at the start of each day were used in the reduction of the data for the test runs of that day. The maximum change in the slope of the calibration curves from day to day was approximately $\pm$ 1% from the arithmetic mean. The non-linearity of the amplifier-transducer circuit produced errors of approximately $\pm$ 1/2% of full scale in the calibration of the transducers. The readability of the data from the oscillograph records resulted in maximum errors of approximately $\pm$ 1/6% of full scale. The errors in measuring static pressures were approximately $\pm$ 1 mm al ($\pm$ 0.06 mm Hg) for the alcohol manometers and $\pm$ 1 mm Hg for the mercury manometer.

CHAPTER IV

THEORY

The equations for the pseudo friction factor are based on the assumptions of one-dimensional, steady, continuum flow, through constant area tubing, with isothermal changes of state. Flow in a tube is normally axially-symmetric with the pressures depending on the radial and longitudinal position. It will be assumed that the radial variations in pressure are small compared to the axial pressure variations; thus, a one-dimensional analysis based on average properties at a cross-section will be used. The assumption of isothermal flow appears reasonable on the grounds that the mass of metal in the system is large compared to the mass flow of air through the system; thus, the metal acts as a sufficiently large heat reservoir to maintain constant temperature. The final equation is obtained by integrating the momentum equation over a small control volume.

Consider the flow of air through the control surface of a long circular tube of constant cross-sectional area shown below.

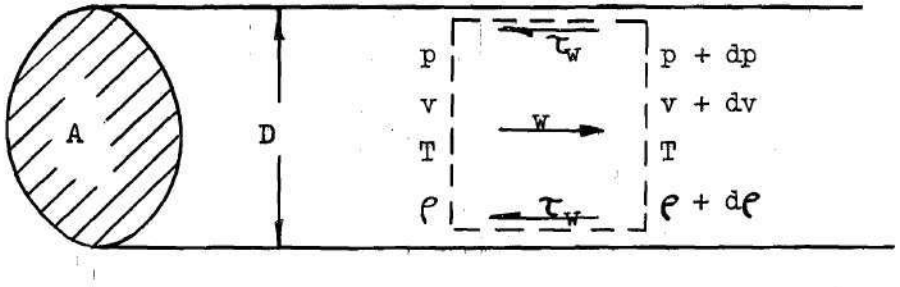

Fig. 3 Control Volume Element

For steady flow through constant area tubing, the continuity equation may be written

$$\frac{w}{A} = \rho v = G, \quad \text{a constant} \tag{IV-1}$$

where w is the rate of mass flow, A is the cross-sectional area of the tubing, ρ is the density of the air, and v is the mean velocity of the air across the section.

Referring to Figure 3 the momentum equation can be written as

$$pA - (p + dp)A - \tau_w\left(\frac{4A}{D}dx\right) = wdv \tag{IV-2}$$

or

$$Adp + \tau_w \frac{4A}{D}\, dx + wdv = 0 \tag{IV-3}$$

where τ_w is the shearing stress exerted on the stream by the walls, $\frac{4A}{D}\, dx$ is the wetted area over which τ_w acts, and p is the static pressure in the tube. The local friction factor is defined by

$$f = \frac{\tau_w}{1/2\ \rho v^2} \tag{IV-4}$$

Introducing f into Equation (IV-3), dividing by A, and multiplying by the density (ρ) yields

$$\rho dp + 1/2(\rho v)^2 \frac{4fdx}{D} + \rho v \frac{w}{A} \frac{dv}{v} = 0 \tag{IV-5}$$

or, substituting for ρ from the perfect gas equation of state $(p = \rho RT)$ and for ρv from the continuity equation gives

$$\frac{pdp}{RT} + \frac{1}{2}\left(\frac{w}{A}\right)^2 \frac{4fdx}{D} + \left(\frac{w}{A}\right)^2 \frac{dv}{v} = 0 \tag{IV-6}$$

Differentiation of the continuity equation yields

$$\frac{dv}{v} + \frac{d\rho}{\rho} = 0 \qquad \text{(IV-7)}$$

Substituting Equation (IV-7) into Equation (IV-6) yields

$$\frac{2pdp}{RT} + \left(\frac{w}{A}\right)^2 \left[\frac{4fdx}{D} - 2\frac{d\rho}{\rho}\right] = 0 \qquad \text{(IV-8)}$$

Under the assumption of isothermal flow, Equation (IV-8) is integrated between the pressures p_I and p_{II} and results in,

$$\frac{p_I^2 - p_{II}^2}{RT} + \left(\frac{w}{A}\right)^2 \left[4\bar{f}\frac{L}{D} - 2\ln\left(\frac{\rho_{II}}{\rho_I}\right)\right] = 0 \qquad \text{(IV-9)}$$

where $\bar{f} = 1/L \int_I^{II} f dx$ is the mean friction factor within the tube, and L is $x_{II} - x_I$. It is to be emphasized that $\bar{f}$ may contain development losses if x_I and x_{II} are taken at the tubing extremities. For isothermal flow, $\rho_I/\rho_{II} = p_I/p_{II}$, and Equation (IV-9) is solved for w as

$$w^2 = \frac{A^2}{RT} \frac{p_I^2 - p_{II}^2}{4\bar{f}\frac{L}{D} + 2\ln(p_I/p_{II})} \qquad \text{(IV-10)}$$

The flow through the system in Figure 4 differs from that of

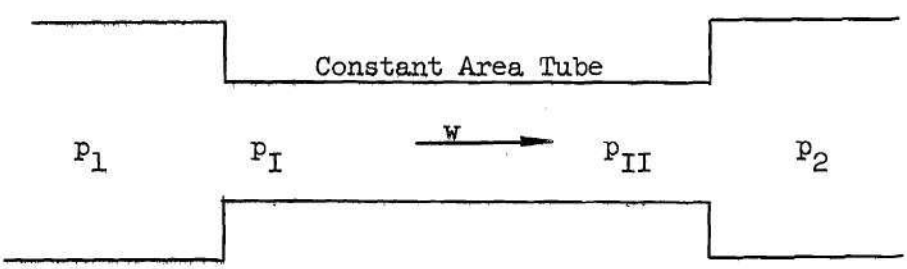

Fig. 4 Equivalent System

Figure 3 in the following respects: the flow is not fully developed over the entire length of tubing, and additional losses occur in the sudden contraction at the entrance to the test tubing and in the sudden expansion at the exit from the test tubing.

Remembering that the data obtained in this study is to be applied to transient flows in systems represented schematically by Figure 1, it is desired to express the mass flow w as a function of p_1 and p_2 (see Fig. 4), rather than as a function of pressures p_I and p_{II} within the test tube. With this idea in mind, define a new friction factor f^* (called a pseudo friction factor) in the following manner:

$$w^2 = \frac{A^2}{RT} \frac{(p_1^2 - p_2^2)}{4f^* \frac{L}{D}} \qquad \text{(IV-11)}$$

Comparing Equation (IV-11) to Equation (IV-10), it is seen that the pseudo friction factor f^* incorporates the compressibility effect ($2 \ln(p_I/p_{II})$, entrance and exit effects, and development effects. Solving explicitly for $4f^*$ yields

$$4f^* = \frac{(p_1^2 - p_2^2)}{\frac{RTL}{D} \left(\frac{w}{A}\right)^2} \qquad \text{(IV-12)}$$

The experimental data taken in this study will be used to determine $4f^*$ from Equation (IV-12).

CHAPTER V

DISCUSSION OF RESULTS

The pseudo friction factors were calculated from Equation (IV-12) using the mass flows as determined by Equation (A-9) in the Appendix. Figures 5 through 8 show the experimental data for the pseudo friction factor ($4f^*$) plotted versus Reynolds number (based on tube inside diameter) for the straight tube case, and for the straight tube with 90, 80, and 70 per cent reduction fittings, respectively. The solid curves are the Hagen-Poiseuille Equation ($4f = 64/Rey$) for laminar flow, and the Karman-Nikuradse curve (Equation I-5) for turbulent flow. The following is a discussion of the results and procedures used to correlate the results for each flow regime.

Laminar Flow Range.--The data in the laminar flow range is seen to be scattered above the Hagen-Poiseuille curve. However, it is to be noted that the experimental points seem to approach the theoretical curve as the Reynolds number approaches 100 for the straight tube with or without reduction fittings. It is supposed that by removing the entrance and exit losses, development losses, and compressibility effect from the pseudo friction factor the true friction factor ($4f$) will be obtained.

From the data of Bradley (8) and Laster (9) the following approximate empirical relations between the pressures inside the pipe and the pressures in the entrance and exit sections are given for the straight tube case by,

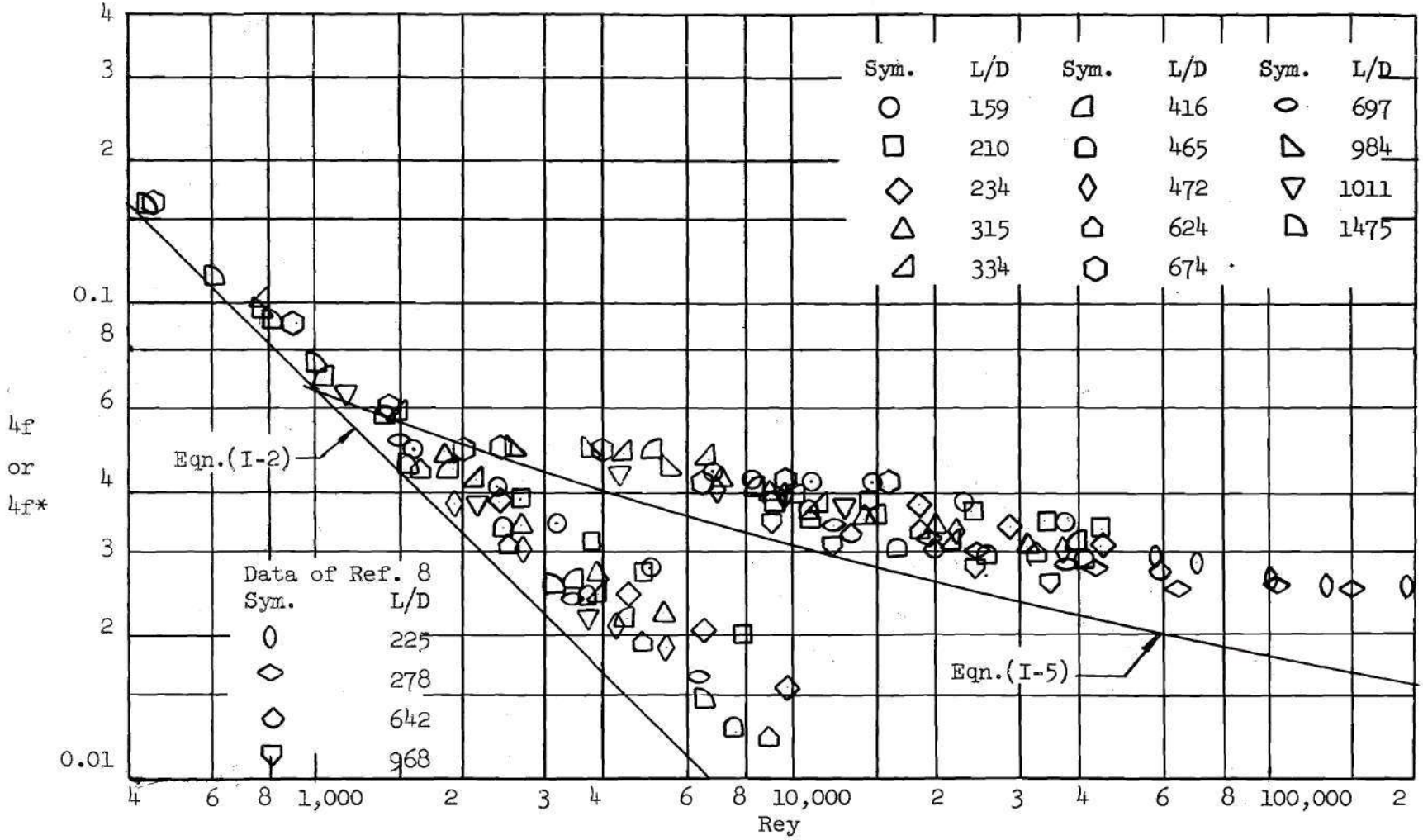

Fig. 5 Pseudo Friction Factor as a Function of Reynolds Number For Straight Tubes

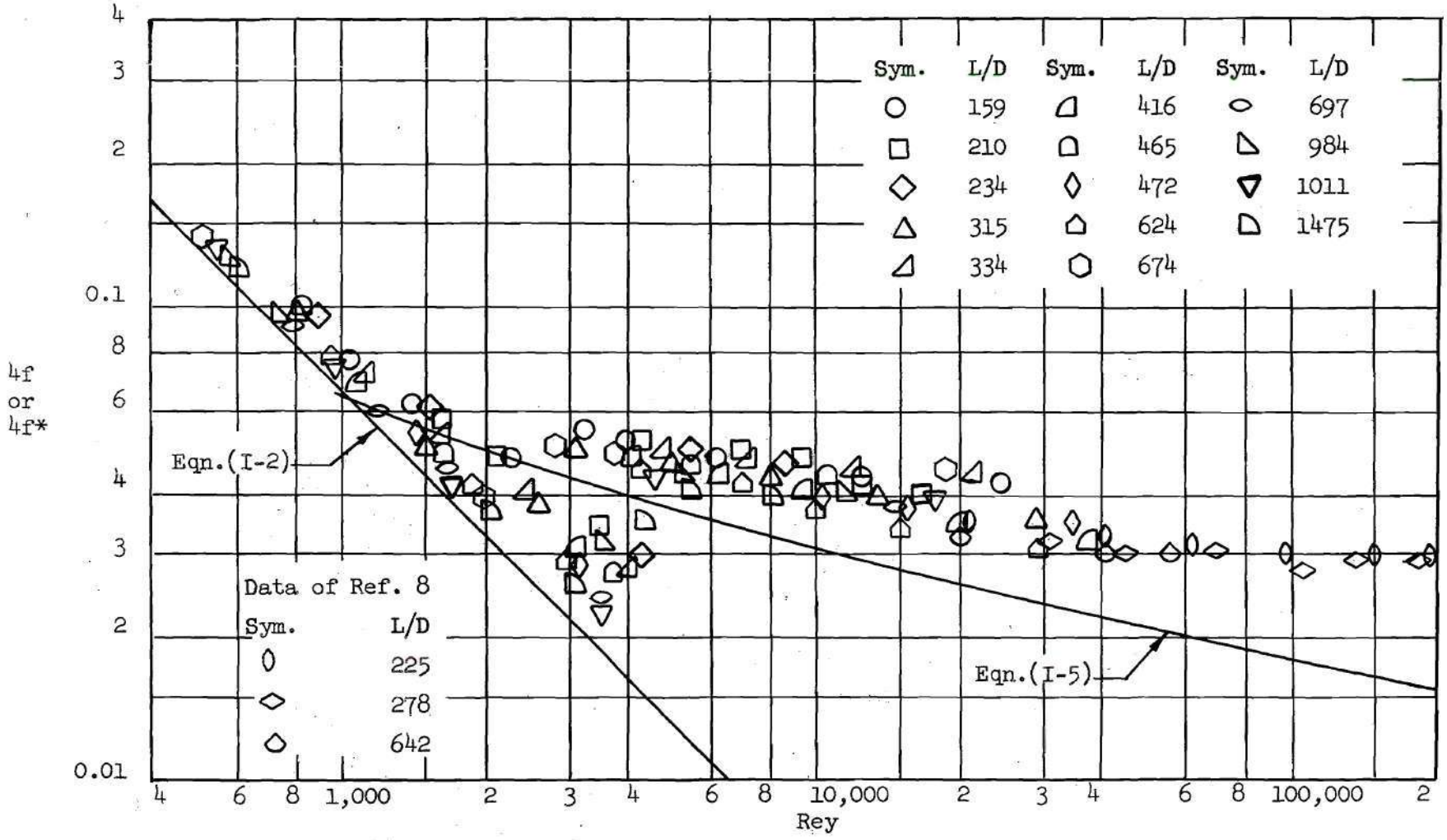

Fig. 6 Pseudo Friction Factor as a Function of Reynolds Number For 90 Per Cent Reduction Fittings

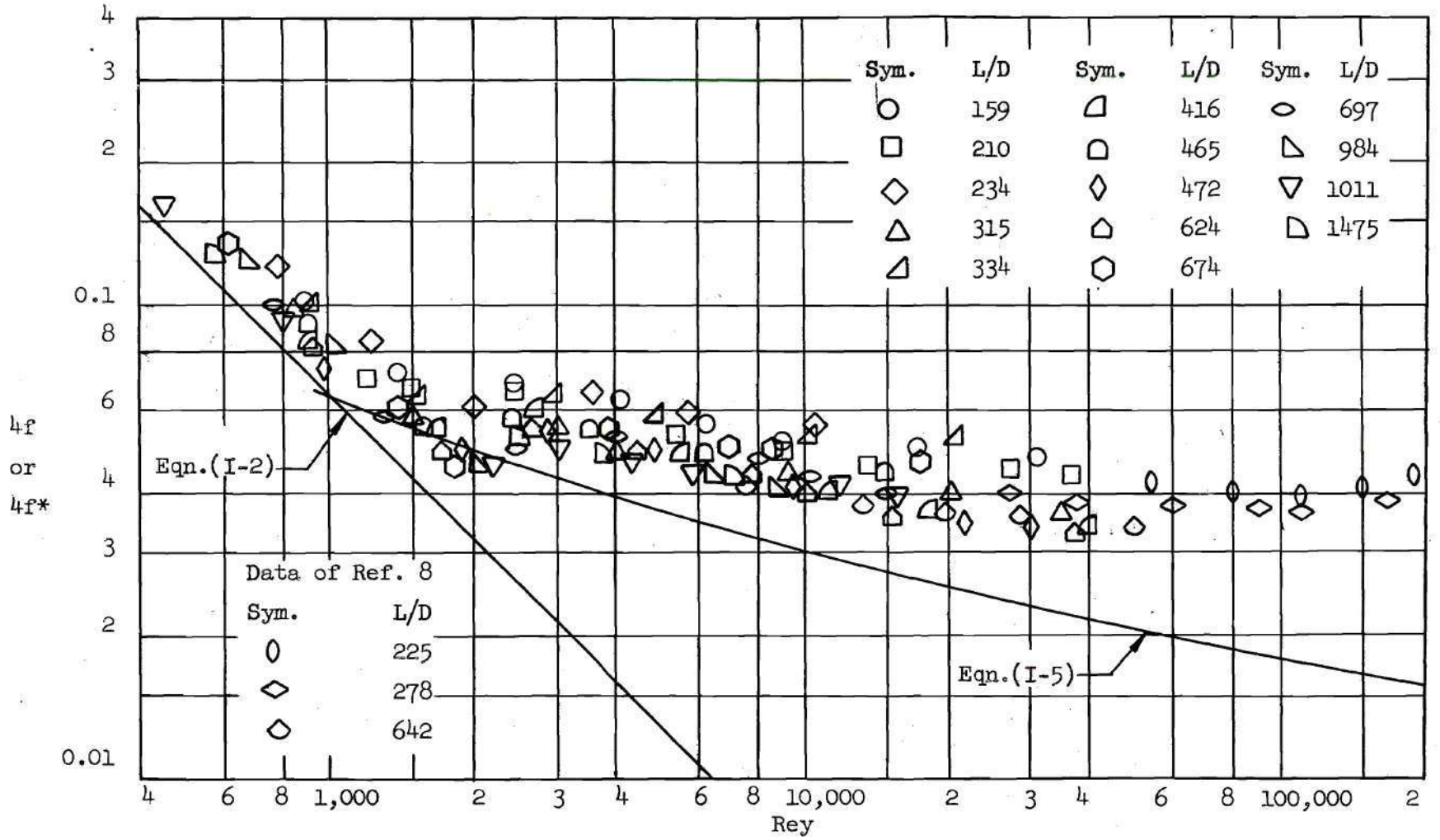

Fig. 7 Pseudo Friction Factor as a Function of Reynolds Number For 80 Per Cent Reduction Fittings

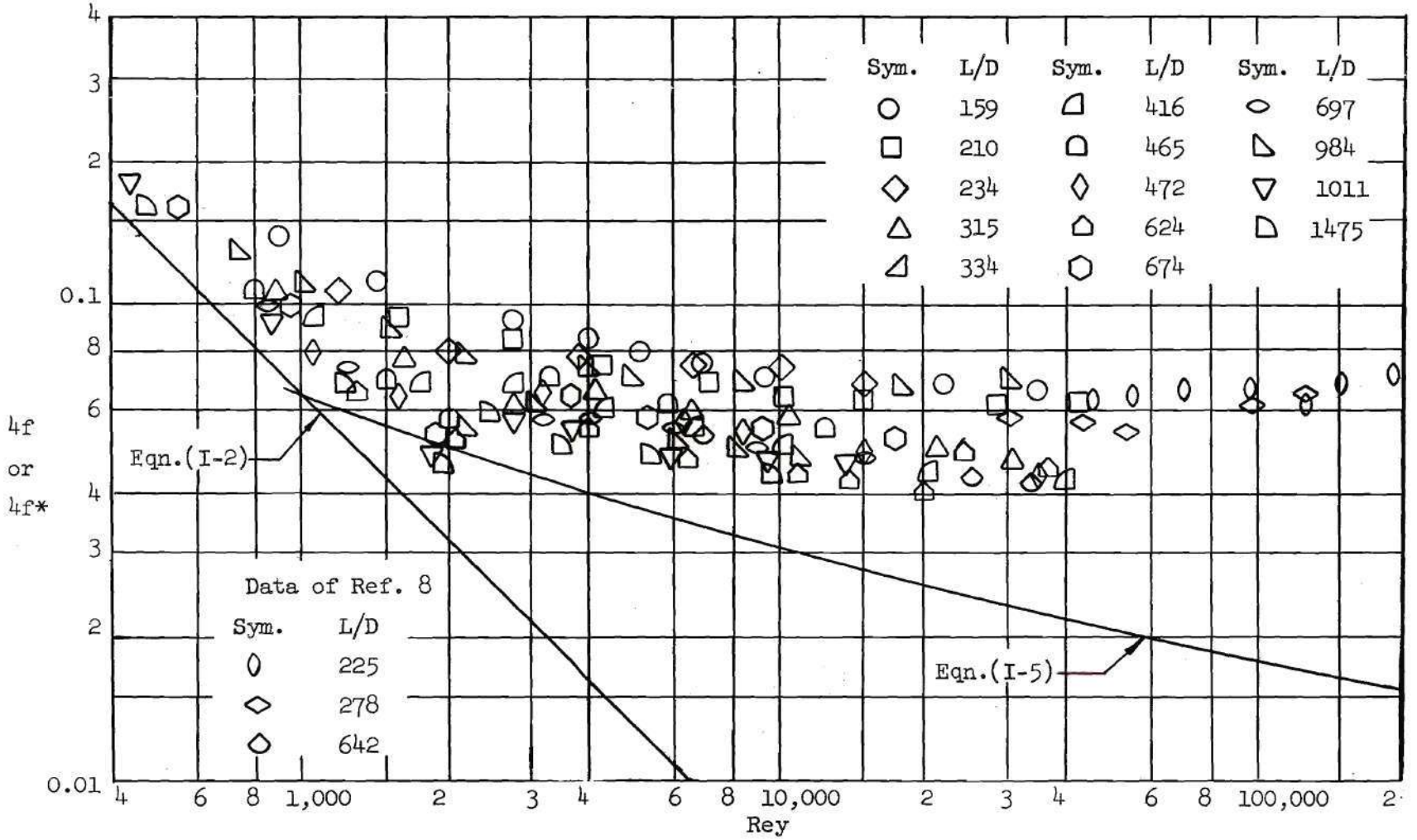

Fig. 8 Pseudo Friction Factor as a Function of Reynolds Number For 70 Per Cent Reduction Fittings

$$p_I \cong p_1(1-1.3\Omega^2) \qquad (V-1)$$

$$p_{II} \cong p_2(1-28\Omega^4) \qquad (V-2)$$

where Ω is a flow factor equal to $G\sqrt{T}/p_1$, given in units of $\sqrt{^\circ R}/sec$. Thus, the inlet and exit pressures (p_1 and p_2, respectively) from Equation (IV-11) can be converted to pressures inside the test tubing (p_I and p_{II}). The entrance and exit losses, and compressibility effects ($\ln p_I/p_{II}$) can now be evaluated. Langhaar (11) showed that the change in friction factor due to development loss is independent of Reynolds number for laminar flow and can be approximated by the term (D/L)(2.28). The true friction factor (4f) can now be obtained for the straight tube case by subtracting these losses from the pseudo friction factor thusly,

$$4f \cong \frac{p_1^2(1 - 1.3\Omega^2)^2 - p_2^2(1 - 28\Omega^4)^2}{\frac{RTL}{D}\left(\frac{w}{A}\right)^2}$$

$$- 2 \ln \left[\frac{p_1(1 - 1.3\Omega^2)}{p_2(1 - 28\Omega^4)}\right] - (D/L)(2.28) \qquad (V-3)$$

For the laminar flows investigated it was found that the flow factor Ω was of the order of 0.01; therefore, the terms $(1 - 1.3\Omega^2)$ and $(1 - 28\Omega^4)$ are approximately unity. Although empirical relations of the form of equations (V-1) and (V-2) were not developed for the straight tubes with reduction fittings, it is supposed that the ratios p_I/p_1 and p_{II}/p_2 are also approximately unity for the laminar flows investigated. Also, it was discovered that the pressure ratio (p_I/p_{II})

was nearly unity. Therefore, $\ln(p_I/p_{II})$ was essentially zero and could be neglected. On the basis of the above arguments the entrance and exit losses and the compressibility effects are neglected. Substituting the relation for $4f^*$ given by Equation (IV-12) into Equation (V-3) results in

$$4f \cong 4f^* - (D/L)(2.28) \qquad (V-4)$$

Thus it is seen that the true friction factor should differ from the pseudo friction factor only by a constant multiplied by the D/L ratio of the tube.

Figures 9 and 10 show the points obtained by Equation (V-4) plotted versus Reynolds number for each of the geometries tested (straight tube, 90, 80, and 70 per cent fittings). The solid line again is the curve of $4f = 64/Rey$. It is now seen that the data has correlated very well but that it still lies above the theoretical curve; therefore,

$$4f \neq 4f^* - (D/L)(2.28) \qquad (V-5)$$

Since all the assumed losses have been removed from the pseudo friction factor the reason for this difference is not known at present.

In view of the above results another friction factor called a correlation friction factor is defined to denote the points plotted in Figures 9 and 10. Thus we have

$$4F \cong 4f^* - (D/L)(2.28) \qquad (V-6)$$

instead of Equation (V-4), where $4F$ is the correlation friction factor.

This correlation friction factor can now be determined empirically

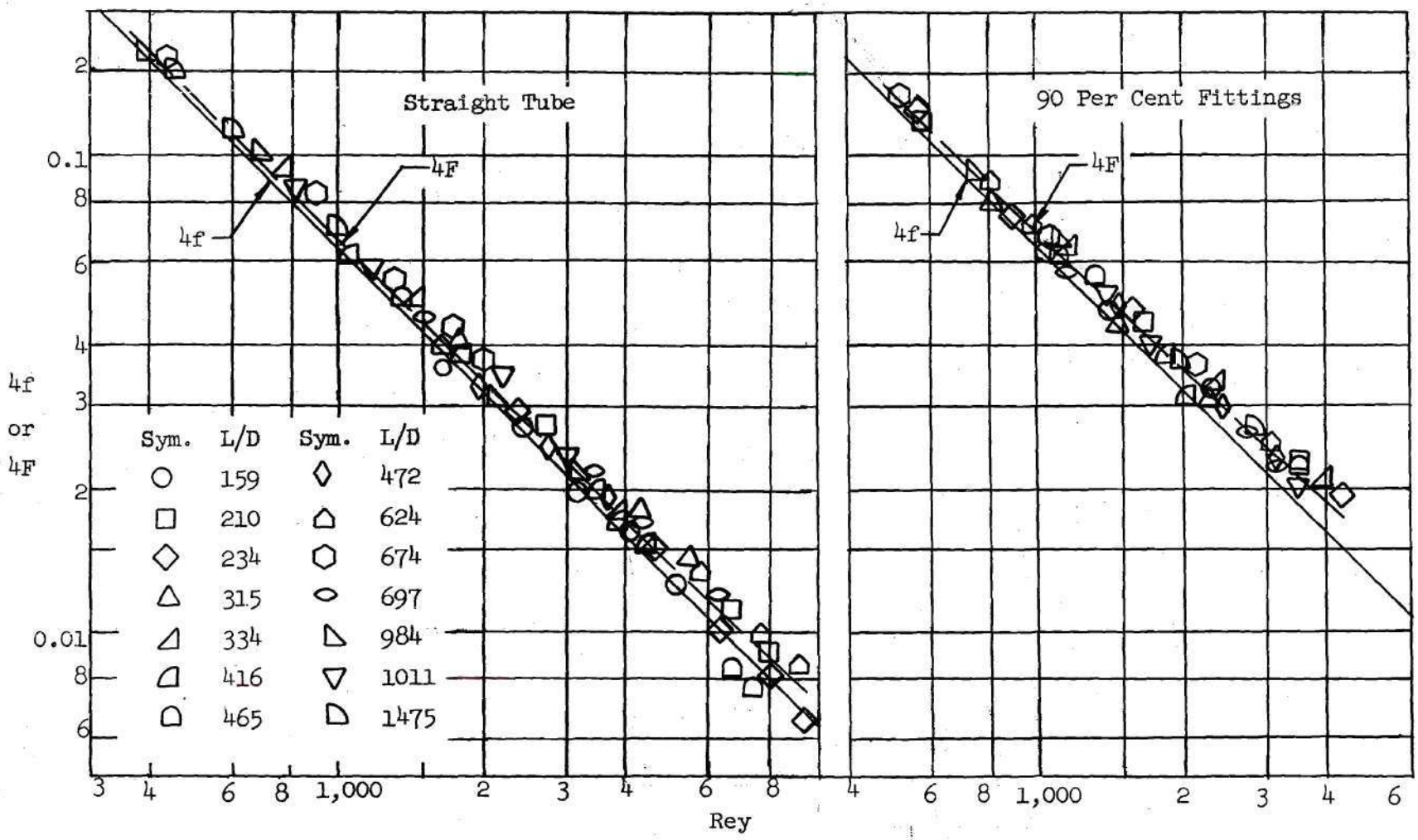

Fig. 9 Correlation of Experiment With Theory For Straight Tube and 90 Per Cent Fitting Data in Laminar Flow Regime

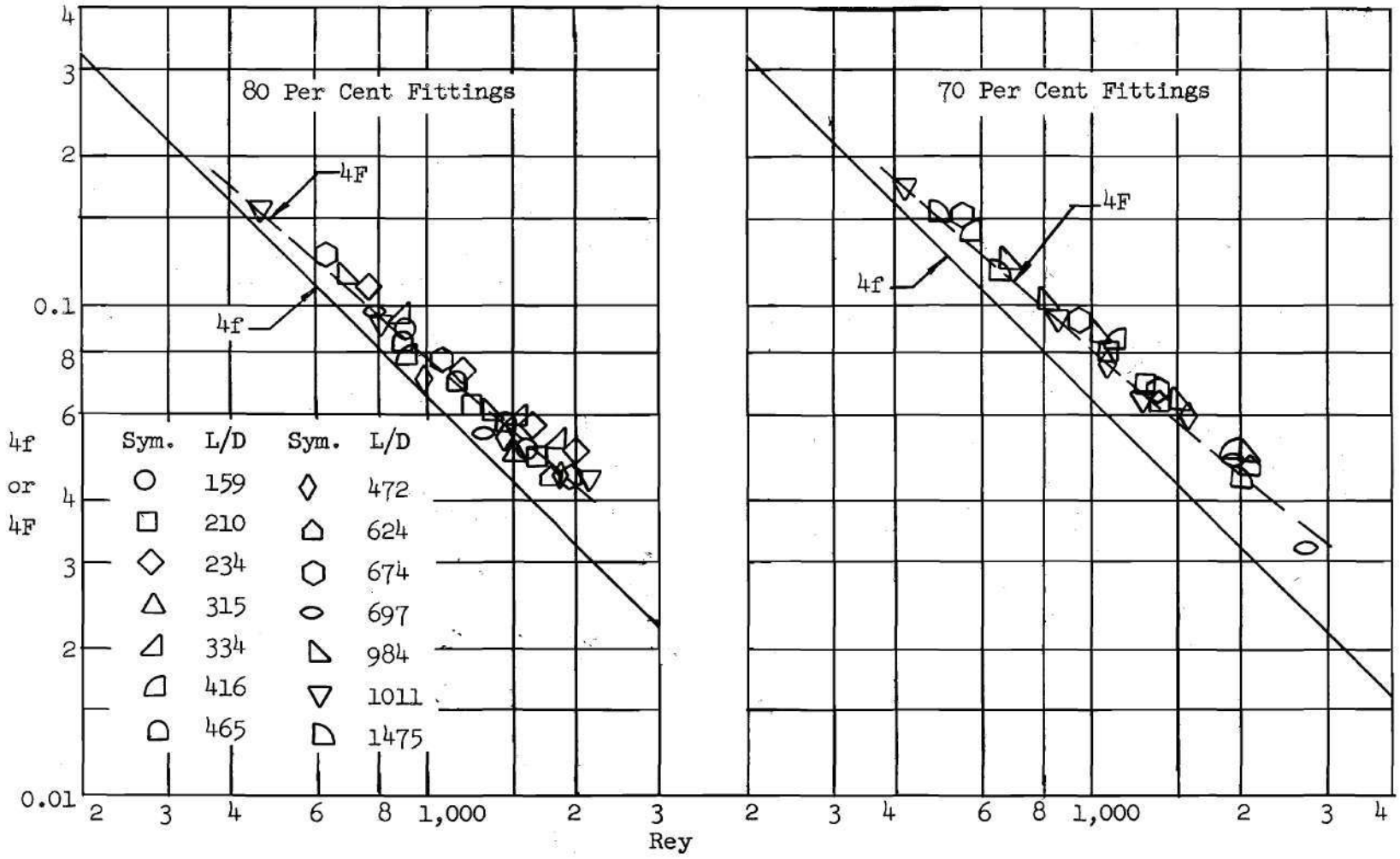

Fig. 10 Correlation of Experiment With Theory For 80 and 70 Per Cent Fitting Data In Laminar Flow Regime

for each case by fairing curves (denoted by dashed lines) through the experimental points in Figures 9 and 10. The following are the empirical relations obtained for approximating $4F$:

straight tube case -

$$4F \cong \frac{64 + 0.2\sqrt{Rey}}{Rey} \qquad (V\text{-}7)$$

90 per cent reduction fittings

$$4F \cong \frac{64 + 0.25\sqrt{Rey}}{Rey} \qquad (V\text{-}8)$$

80 per cent reduction fittings

$$4F \cong \frac{64 + 0.5\sqrt{Rey}}{Rey} \qquad (V\text{-}9)$$

70 per cent reduction fittings

$$4F \cong \frac{64 + 0.8\sqrt{Rey}}{Rey} \qquad (V\text{-}10)$$

The desired relation for the pseudo friction factor can now be determined. For a given tube (given L/D ratio) the pseudo friction factor can be computed from the known relation for $4F$ thusly,

$$4f^* \cong 4F + (D/L)(2.28) \qquad (V\text{-}11)$$

The right hand side of Equation (V-11) can now be plotted versus Reynolds number and then approximated, over a moderate range of pressure ratios, by a relation $C(Rey)^{-n}$.

The advantage of this semi-empirical approach through $4f^*$ lies in the simplicity of the resulting quasi-steady state equation, (I-6). On the other hand, direct use of the friction factors as given by Equa-

tions (V-7) through (V-10) would result in a cumbersome implicit expression for the time rate of change of response pressure.

Turbulent Flow Regime.--The data in the turbulent flow regime (Figures 5 through 8) is seen to scatter above the Karman-Nikuradse curve. Experimental points obtained from Bradley's data are also plotted in Figures 5 through 8 and show relatively good agreement with the data obtained in this experiment. The data is correlated by subtracting from the pseudo friction factor ($4f^*$), in a manner similar to that used for the laminar flow case, all the losses other than those attributable to fully-developed turbulent friction.

A relation similar to Equation (V-3) is obtained for the straight tube (100 per cent) case, except that a different term is needed to account for the change in friction factor due to development losses. The theoretical work of Deissler (12) indicates that this term might be approximated by (27,000/Rey)(D/L). The resulting equation for $4f$ applicable to turbulent flow is

$$4f \cong \frac{p_1^2(1 - 1.3\Omega^2)^2 - p_2^2(1 - 28\Omega^4)^2}{\frac{RTL}{D}\left(\frac{W}{A}\right)^2}$$

$$- \left(\frac{D}{L}\right) 2 \ln \left[\frac{p_1(1 - 1.3\Omega^2)}{p_2(1 - 28\Omega^4)}\right] - (D/L)(27,000/Rey) \qquad (V\text{-}12)$$

Equation (V-12) is only valid for the straight tube case in turbulent flow since no correlation for accounting for the end effects with reduction fittings has been developed in this study. Equation (V-12) differs from Equation (V-3) in that the flow factor, Ω , and the ln

(p_1/p_2) are no longer small. Therefore, the entrance and exit losses and compressibility effect cannot be neglected.

Figure 11 shows the results of applying Equation (V-12) to the turbulent data in Figure 5. The solid curve represents the Karman-Nikuradse curve (Equation I-5) and the data is seen to scatter about this curve. The scatter is within $\pm$ 7% thus indicating that the correlation is adequate.

In order to obtain a pseudo friction factor a value of G ($= \frac{W}{A}$) must be determined to use in Equation (IV-12). This value of G is obtained by solving Equation (V-12) by iteration in the following manner. For a given p_1, p_2, T, D, and L, a value of G is assumed (enabling a Reynolds number and μ to be computed), and the equation solved for $4f$. By using this value of $4f$ in the Karman-Nikuradse Equation (I-5) a Reynolds number and thereby a value of G can be computed. This procedure is repeated until the value of G assumed in Equation (V-12) and that calculated from Equation (I-5) converge to the desired accuracy. After G is obtained the pseudo friction factor $4f^*$ can be obtained from Equation (IV-12). Then, for a given tube, $4f^*$ can be plotted versus Reynolds number and approximated by a relation such as Equation (I-1). As seen previously the quasi-steady state equation (I-6) can now be readily solved by numerical methods.

Since no procedure for obtaining pseudo friction factors for tubes with fittings in turbulent flows was developed, a qualitative method is now suggested. For a given tube and fitting size a straight line can be faired through the appropriate points in Figure 6, 7, or 8 and a relation $C(Rey)^{-n}$ thus obtained for the range of pressure ratios

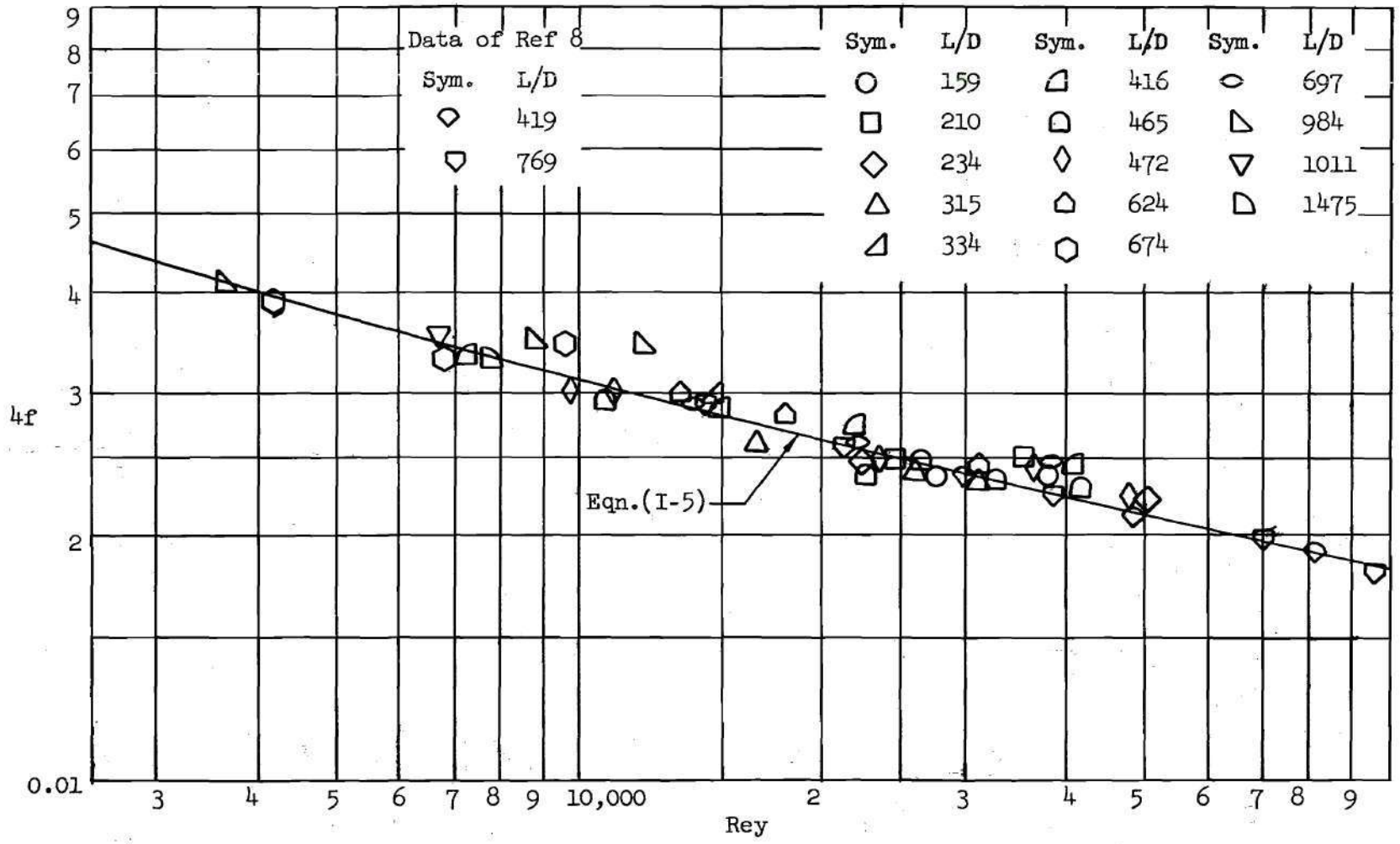

Fig. 11 Correlation of Experiment With Theory For Straight Tube Data In Turbulent Flow Regime

tested.

Effect of Reduction Fittings.--Figures 12 and 13 show the effect of reduction fittings for a high L/D ratio (1011) and a low L/D ratio (159) respectively. At a given Reynolds number the pseudo friction factor is seen to increase with a decrease in fitting diameter because of the fact that a smaller size fitting would necessarily have larger inlet and exit losses, and probably a greater development loss. A decrease in fitting diameter is also seen to cause the flow to change from laminar to turbulent at a lower Reynolds number.

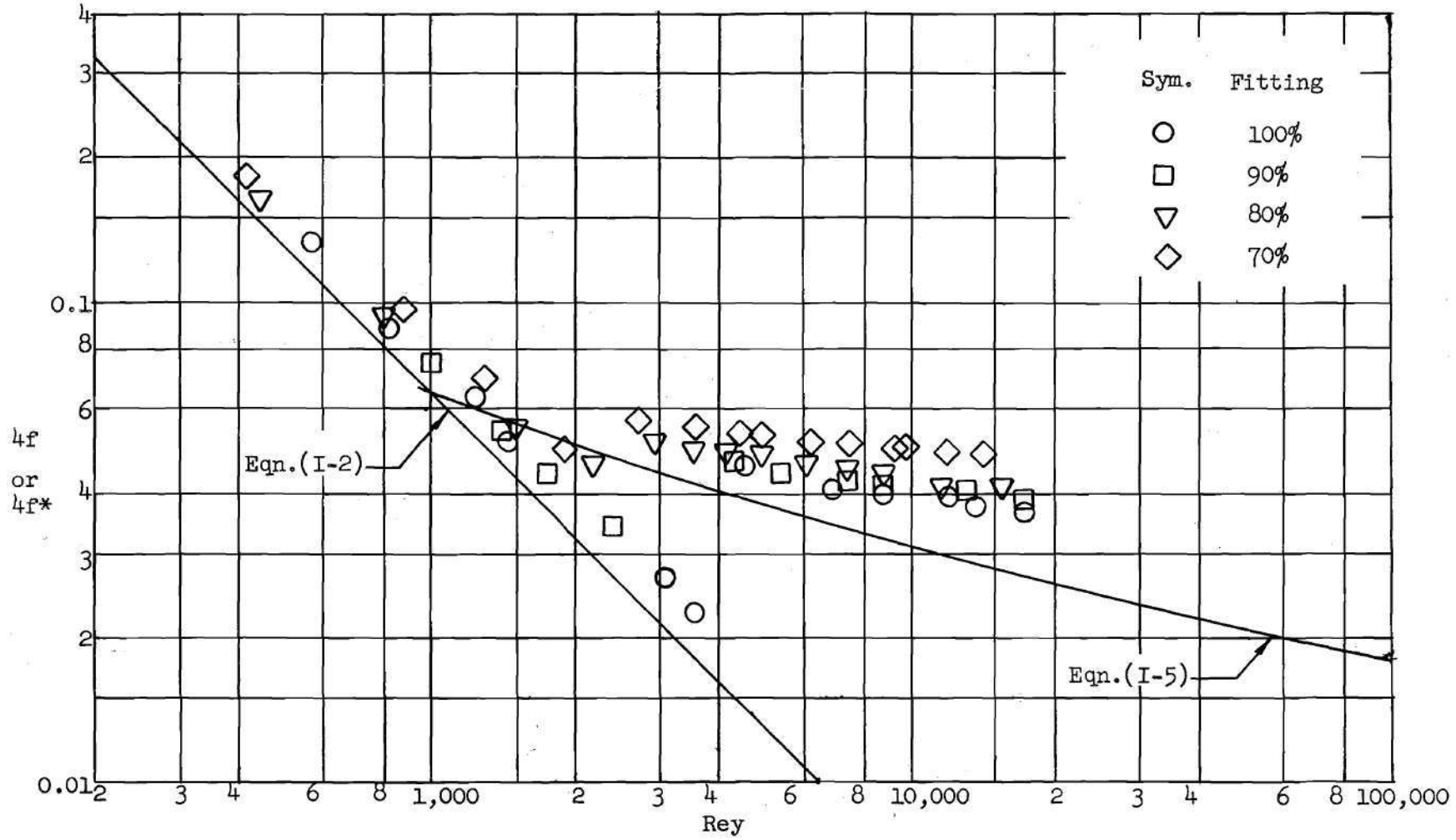

Fig. 12 Pseudo Friction Factor as a Function of Reynolds Number For L/D = 1011 Showing Effect of Reduction Fittings

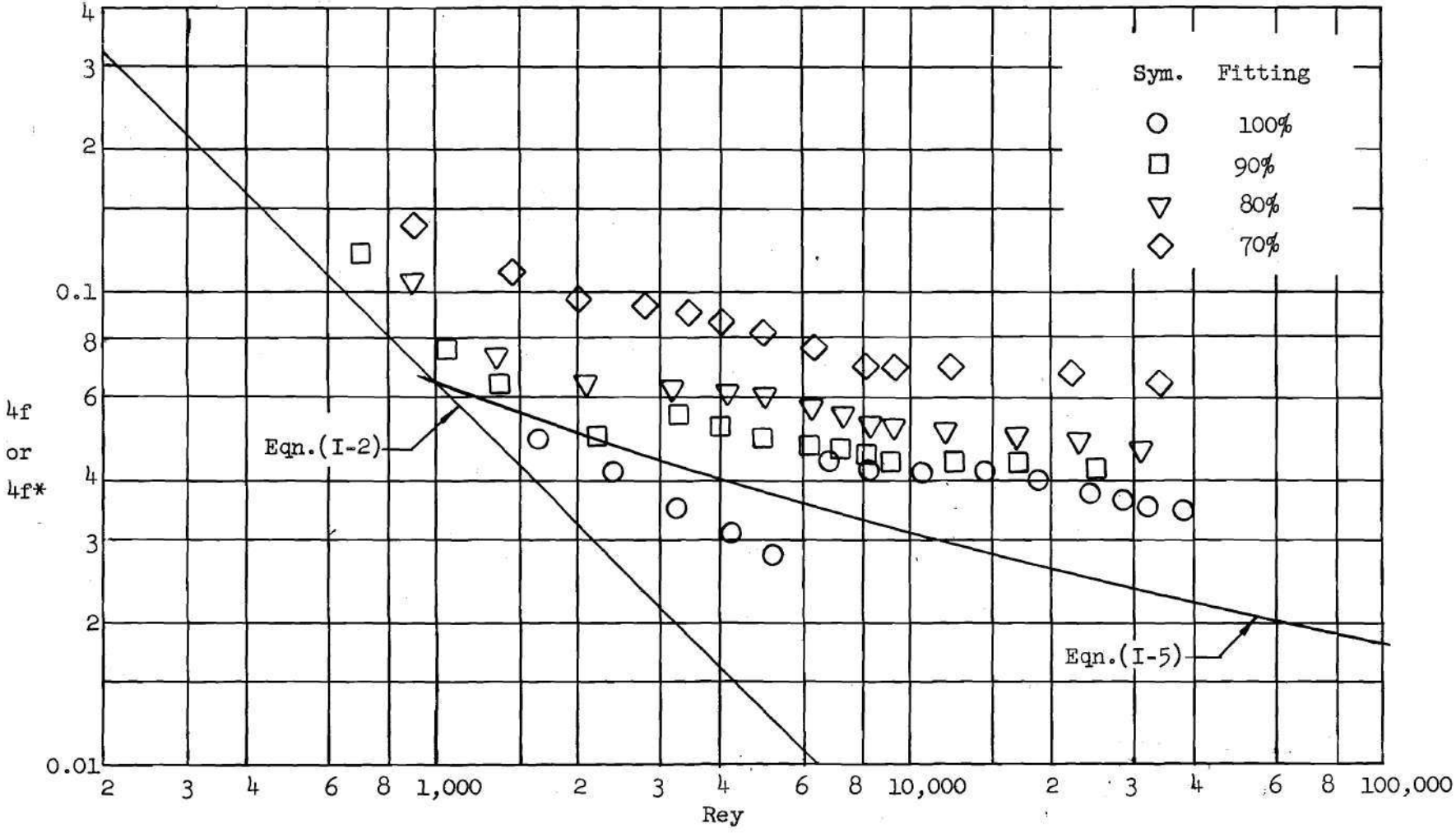

Fig. 13 Pseudo Friction Factor as a Function of Reynolds Number For L/D = 159 Showing Effect of Reduction Fittings

CHAPTER VI

CONCLUSIONS

The results of this investigation are limited to tube lengths from 5 to 15 feet, tube diameters from 0.122 to 0.384 inches, and reduction fittings from 100 to 70 per cent. The results are also limited to experiments run at room temperature with the downstream pressure held constant at atmospheric pressure, and Reynolds numbers ranging between 400 and 50,000.

From the results of this experiment, subject to the limitations listed, it can be concluded that:

1. For the laminar flow regime (straight tube with or without reduction fittings),

a. The pseudo friction factor approaches the Hagen-Poiseuille curve as the Reynolds number approaches 100.

b. By removing the entrance and exit effects, compressibility effects, and development losses from the pseudo friction factor, the data can be correlated but still lies above the Hagen-Poiseuille curve.

c. The pseudo friction factor can be computed from

$$4f^* \cong 4F + (D/L)(2.28) \qquad (V\text{-}11)$$

where $4F$ can be determined empirically from the following relations:

straight tube -

$$4F \cong \frac{64 + 0.2\sqrt{Rey}}{Rey} \qquad (V\text{-}7)$$

90 per cent fittings -

$$4F \cong \frac{64 + 0.25\sqrt{Rey}}{Rey} \qquad (V\text{-}8)$$

80 per cent fittings -

$$4F \cong \frac{64 + 0.5\sqrt{Rey}}{Rey} \qquad (V\text{-}9)$$

70 per cent fittings -

$$4F \cong \frac{64 + 0.8\sqrt{Rey}}{Rey} \qquad (V\text{-}10)$$

d. For a given L/D ratio, the constants C and n to be used in the quasi-steady theory can be determined from the relation

$$4f^* = C(Rey)^{-n} \qquad (I\text{-}7)$$

2. For the turbulent flow regime,

a. The data obtained agrees with experimental data obtained previously by Bradley.

b. For the straight tube case the pseudo friction factor can be correlated to the Karman-Nikuradse curve by removing the entrance and exit effects, development losses, and compressibility effects.

c. By solving the equation

$$4f \cong \frac{p_1^2(1 - 1.3\Omega^2)^2 - p_2^2(1 - 28\Omega^4)^2}{\frac{RTL}{D}\left(\frac{w}{A}\right)^2}$$

$$- (D/L)\, 2 \ln \left[\frac{p_1(1 - 1.3\Omega^2)}{p_2(1 - 28\Omega^4)}\right] - (D/L)(27{,}000/Rey) \qquad (V\text{-}12)$$

by integration to obtain $\frac{W}{A}$, where $4f$ is given by the Karman-Nikuradse relation,

$$1/\sqrt{4f} = 2.0 \log_{10}(\text{Rey}\sqrt{4f}) - 0.8 \qquad \text{(I-5)}$$

the pseudo friction can be computed from

$$4f^* \cong \frac{p_1^2 - p_2^2}{\frac{RTL}{D}\left(\frac{W}{A}\right)^2} \qquad \text{(IV-12)}$$

for the straight tube case. The constants C and n for a given tube can again be obtained from the relation

$$4f^* = C(\text{Rey})^{-n} \qquad \text{(I-7)}$$

d. A relation of the form

$$4f^* = C(\text{Rey})^{-n} \qquad \text{(I-7)}$$

can be obtained qualitatively for the 90, 80, and 70 per cent reduction fittings by fairing a straight line through the data points for a given tube and given fitting size.

3. For a given Reynolds number a decrease in fitting diameter is seen to increase the pseudo friction factor. Also a fitting diameter decrease tends to lower the transition Reynolds number.

CHAPTER VII

RECOMMENDATIONS

In order to extend the experimentation for obtaining friction factors in small bore tubing, the following recommendations are made:

1. Additional data should be obtained for the range of Reynolds numbers from 100 to 500, since this range contains the least accurate data in this experiment.

2. A procedure for correlating the end effects for tubes with reduction fittings should be determined for turbulent flow.

3. The effects of inlet temperatures different from room temperatures should be determined.

4. The effects of pressure levels different from atmospheric should be investigated both experimentally and theoretically.

A P P E N D I X

APPENDIX

DEVELOPMENT OF THE BASIC FLOW EQUATION THROUGH A SHARP-EDGED ORIFICE

Following the procedure outlined by the ASME (10) it is assumed that the flow through the metering orifice is steady, incompressible, and obeys the perfect gas laws. In addition, the assumption is made that there is no loss of energy from friction and no heat transfer takes place between the fluid and the surrounding walls.

Consider the stations 1 and 2 in the element shown in Figure 14.

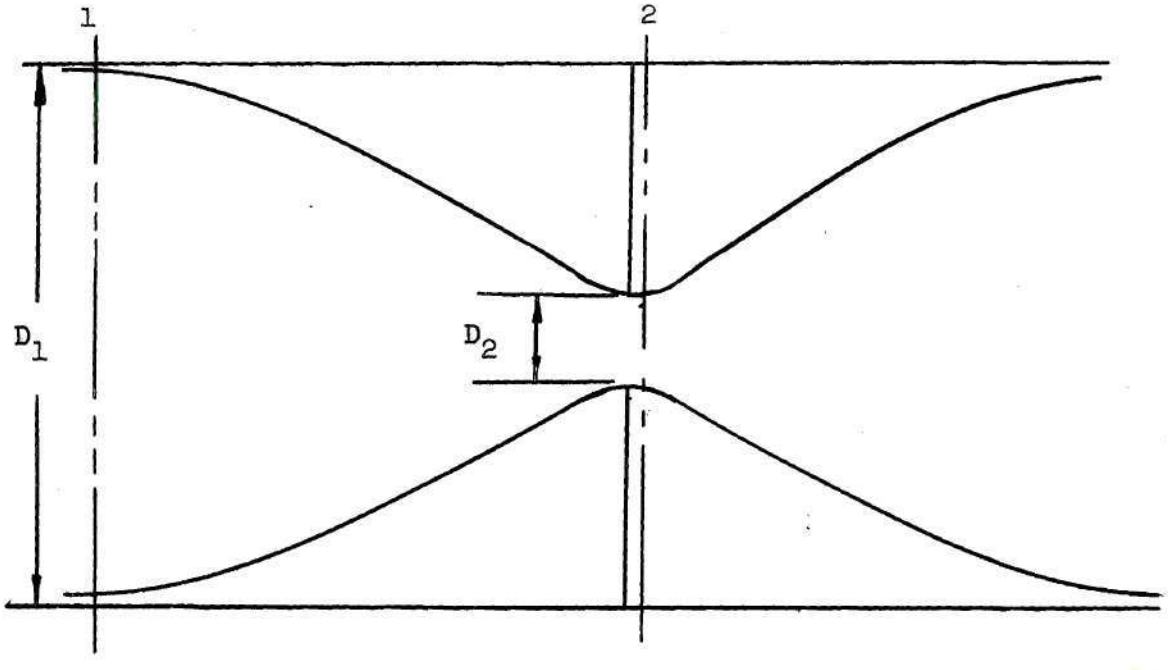

Fig. 14 Metering Element

The incompressible Bernoulli equation gives

$$P_1 + \frac{\rho V_1^2}{2g} = P_2 + \frac{\rho V_2^2}{2g} \qquad \text{(A-1)}$$

where P_1, V_1, P_2, V_2 are pressure and velocity at stations 1 and 2 respectively, ρ is the density, and g is the acceleration due to gravity.

Rearranging gives

$$(V_2^2 - V_1^2)\frac{\rho}{2g} = P_1 - P_2 = \Delta P \qquad \text{(A-2)}$$

From continuity considerations the rate of flow, w, is given by

$$w = \rho A_1 V_1 = \rho A_2 V_2 \qquad \text{(A-3)}$$

where A_1 and A_2 are the cross-sectional areas at stations 1 and 2 respectively.

Analyzing the circular cross section gives

$$w = \rho V_1 \frac{\pi D_1^2}{4} = \rho V_2 \frac{\pi D_2^2}{4} \qquad \text{(A-4)}$$

or

$$V_1 = V_2 \left(\frac{D_2}{D_1}\right)^2 = V_2 B^2 \qquad \text{(A-5)}$$

where B is the ratio of orifice diameter to pipe diameter, $\frac{D_2}{D_1}$. Substituting (A-5) into (A-2) and simplifying results in

$$V_2 = \frac{1}{\sqrt{1 - B^4}} \sqrt{\frac{2g \Delta P}{\rho}} \tag{A-6}$$

It follows from the equation of state ($P_1 = \rho RT_1$) and Equation (A-3) that

$$w = \frac{A_2}{\sqrt{1 - B^4}} \sqrt{\frac{2gP_1 \Delta P}{RT_1}} \tag{A-7}$$

Since the actual flow varies from the above theoretical relations the ASME suggests three empirical corrections (K, Y, E) to the above equation. The discharge coefficient K is a function of Reynolds number, the compressibility factor Y is a function of the B ratio and the pressure ratio, and E is a coefficient which corrects for the thermal expansion of the metering element.

Now for air the flow rate, w, is given by

$$w = 1.10 \frac{A_2 K Y E}{\sqrt{1 - B^4}} \sqrt{\frac{P_1 \Delta P}{T_1}} \tag{A-8}$$

Before applying Equation (A-8) to the data in this experiment, one notes that for $B = 0.1$ and 0.05 the factor $\sqrt{1 - B^4}$ is essentially unity. In addition, the factor E is equal to unity for room temperature. Finally, for isothermal flow $P/T = \rho R$. Equation (A-8) now becomes

$$w = 1.10 A_2 K Y \sqrt{R \rho \Delta P} \tag{A-9}$$

REFERENCES

1. Karman, T. von, Mechanical Similitude and Turbulence, National Advisory Committee for Aeronautics, Technical Memorandum 611, 1931.

2. Nikuradse, J., Gesetzmabigkeiten der Turbulenten Strömung in glatten Rohren, Forschungs-Arb. Ing.-Wesen, No. 356, 1932.

3. Schlicting, H., Boundary Layer Theory, Trans., Kestin, J., New York: McGraw-Hill Book Co., Inc., 1955, pp. 400-406.

4. Ibid, p. 63.

5. Blasius, H., Das Ähnlichkeitsgesetz bei Reibungsvorgangen in Flussigkeiten, Forschurgs-Arb. Ing.-Wesen, No. 131, Berlin, 1913.

6. Drew, T. B., Koo, E. C., and McAdams, W. H., "Friction Factors for Clean Round Pipes", Transactions American Institute of Chemical Engineers, 28-56, 1932.

7. Stone, G. W., Transient Response Characteristics of Simulated Missile Pneumatic Plumbing Systems Subjected to Shock Wave Inputs, Unpublished Master's Thesis, Georgia Institute of Technology, 1960.

8. Bradley, R. G., An Experimental Investigation of Air Flow Through Insulated Tubing as a Function of Approach Temperature, Pressure Ratio, Length, and Diameter, Unpublished Master's Thesis, Georgia Institute of Technology, 1957.

9. Laster, M. L., A Theoretical and Experimental Analysis of Lengthwise Pressure Gradient for Flow of Air in Small Bore Tubing Considering the Effect of Elevated Temperature, Unpublished Master's Thesis, Georgia Institute of Technology, 1958.

10. "Fluid Meters, Their Theory and Application, Part I"; The American Society of Mechanical Engineers, 1937.

11. Langhaar, H. L., "Steady Flow in Transition Length of Straight Tube"; Transactions of the American Society of Mechanical Engineers, 64: A-55, 1942.

12. Deissler, R. G., Analysis of Turbulent Heat Transfer and Flow in the Entrance Regions of Smooth Passages, National Advisory Committee for Aeronautics, Technical Note 3016, 1953.